
Article:
Yang, L., Neild, S.A., Wagg, D.J. et al. (2006) Model reference adaptive control of a nonsmooth dynamical system. Nonlinear Dynamics, 46 (3). 323 - 335. ISSN: 0924-090X

https://doi.org/10.1007/s11071-006-9048-6

Model reference adaptive control of a nonsmooth dynamical system

July 5, 2014

L. Yang, S.A. Neild*, D.J. Wagg and D.W. Virden

Department of Mechanical Engineering, University of Bristol, Queens Building, University Walk,

Bristol BS8 1TR, U.K. *Author for correspondence(e-mail:Simon.Neild@bristol.ac.uk; fax:+44-117-929-4423)

Citation: *Nonlinear Dynamics 46:323-335 Article number 3, 2006.*

Abstract

In this paper a modified model reference adaptive control (MRAC) technique is presented which can be used to control systems with nonsmooth characteristics. Using unmodified MRAC on (noisy) nonsmooth systems leads to destabilization of the controller. A localized analysis is presented which shows that the mechanism behind this behavior is the presence of a time invariant zero eigenvalue in the system. The modified algorithm is designed to eliminate this zero eigenvalue, making all the system eigenvalues stable. Both the modified and unmodified strategies are applied to an experimental system with a nonsmooth deadzone characteristic. As expected the unmodified algorithm cannot control the system, whereas the modified algorithm gives stable robust control, which has significantly improved performance over linear fixed gain control.

Keywords: Gain wind-up, Non-smooth dynamics, Adaptive control, Robustness.

Running title: MRAC of a nonsmooth system

1 Introduction

In this paper a model reference adaptive control (MRAC) technique is presented which can be applied to non-smooth systems. This is significant because, although MRAC type controllers have been applied to nonlinear systems [1–9], the presence of nonsmooth dynamics typically destabilizes these controllers [10, 11]. The technique presented here is in fact a modification to the standard MRAC approach — descriptions of the standard approach can be found in a range of textbooks, for example [12–14]. The modified algorithm is applied to an experimental system with a nonsmooth 'dead zone' characteristic and shown to give stable and robust control.

The modified algorithm is developed by considering the MRAC system as a set of three nonlinear ordinary differential equations (ODE's). The concept of studying these type of systems as sets of ODE's has been considered by (amongst others) [14–19]. In this work, the behavior of a single input, single output (SISO) model reference control system, is studied using a state space, dynamical systems approach as typified by [20]. The resulting dynamical system is strongly nonlinear and has a particular structure consistent with adaptive systems which results in a zero eigenvalue in the Jacobian of the linearized system for all parameter values (see [21] and references therein for similar observations on related adaptive systems). By studying the dynamics of the localized system (see for example [22–24]) it can be demonstrated that an infinite number of fixed points exist for the system, and that for a unit step demand they form a time invariant *exact matching manifold*. The (global) dynamics along the exact matching manifold can also be obtained by projecting the system onto a basis formed by the eigenvectors of the linearized system using a center manifold projection [20], an approach previously used to study another class of adaptive control systems [21].

From a practical viewpoint, the robustness of the system to 'gain wind-up' (sometimes called 'drift' or 'creep') is of key importance. For unmodified MRAC, the presence of a zero eigenvalue means that some disturbance signals can be enough to induce gain wind-up — although persistence of excitation also plays a role in this process [14]. The presence of nonsmooth discontinuities exacerbates this wind-up process [11]. Therefore a modified algorithm is presented which eliminates the zero eigenvalue, so that the system can be shown to be both locally and globally asymptotically stable for a selected class of control demand signals [25]. It is worth noting that other modifications to MRAC have been presented (for example [26]). The modification presented here is similar to the gain "leakage" strategies, which have been applied to integral only adaptive gain strategies [27,28]. However, the localized stability analysis of system [25] shows theoretically why

these modifications give the system improved stability and robustness. The nonsmooth experimental example presented in Section 4.2 gives a graphic illustration of this.

2 Theoretical formulation of the MRAC algorithm

In this section a brief review of the MRAC method is given for a SISO system. For more detailed discussions of MRAC see [12–14] and references therein and Appendix A1.

The system studied in this paper is based on a first-order linear plant approximation given by

$$\dot{x}(t) = -ax(t) + bu(t) \tag{1}$$

where $x(t)$ is the plant state, $u(t)$ is the control signal and a and b are the plant parameters. The control signal is generated from both the state variable and the reference (or demand) signal $r(t)$, multiplied by the adaptive control gains K and K_r, such that

$$u(t) = K(t)x(t) + K_r(t)r(t), \tag{2}$$

where, $K(t)$ is the feedback adaptive gain and $K_r(t)$ the feed forward adaptive gain. The plant is controlled to follow the output from a reference model

$$\dot{x}_m(t) = -a_m x_m(t) + b_m r(t), \tag{3}$$

where x_m is the state of the reference model and a_m and b_m are the reference model parameters which are specified by the controller designer. The object of the MRAC algorithm is for $x_e \to 0$ as $t \to \infty$, where $x_e = x_m - x$ is the error signal. The dynamics of the system may be rewritten in terms of the error such that

$$\dot{x}_e(t) = -a_m x_e(t) + (a - a_m - bK(t))\, x(t) + (b_m - bK_r(t))\, r(t). \tag{4}$$

Using Equations (1), (2) and (3), it can be seen that for exact matching between the plant and the reference model, the following relations hold

$$K = K^E = \frac{a - a_m}{b}, \tag{5}$$

$$K_r = K_r^E = \frac{b_m}{b}. \tag{6}$$

where $()^E$ denotes the (constant) Erzberger gains [15]. Equations (5) and (6) can be used to express Equation (4) as

$$\dot{x}_e = -a_m x_e + b(K^E - K)(x_m - x_e) + b(K_r^E - K_r)r. \tag{7}$$

A generic objective of model reference adaptive control is to adapt to minimize the error x_e without detailed knowledge of the plant parameter values a and b. Usually this takes place in the presence of plant uncertainties, and in this case a and b are scalars based (and $b > 0$) on the assumption that the plant has first-order dynamics. As a result the objective is not to explicitly solve Equation (7), (which is based on a first-order plant approximation) but provide a controller which can cope with as large a range of a and b values as possible.

For general model reference adaptive control, the adaptive gains are commonly defined in a proportional plus integral formulation

$$K(t) = \alpha \int_0^t y_e x(\tau) \mathrm{d}\tau + \beta y_e x(t) + K_0, \tag{8}$$

$$K_r(t) = \alpha \int_0^t y_e r(\tau) \mathrm{d}\tau + \beta y_e r(t) + K_{r0}, \tag{9}$$

where α and β are adaptive control weightings representing the adaptive effort and K_0 and K_{r0} are the initial gain values. Experimentally, it has been found that the ratio $\alpha/\beta = 10$ works well [4]. In higher order MRAC implementations, y_e is a scalar weighted function of the error state and its derivatives, $y_e = C_e x_e$, where C_e can be chosen to ensure the stability of the feed forward block [12] (see also Appendix A1). In the case of a first-order implementation, C_e is a scalar and therefore may be incorporated into the α and β adaptive control weightings.

In general, it is usual to use estimates of the Erzberger gains, based on a first-order system identification of the plant, as the initial gain values, K_0 and K_{r0}. Alternatively the initial gain values may be set to zero such that the controller requires no knowledge of the plant parameters a and b [4] — although this generally leads to slower convergence to final gain values. The adaptive weightings, α and β need to be selected in advance, and clearly have a significant influence on the rate of adaptation as they act as fixed gain values which multiply the proportional and integral parts of the controller gain. How to select appropriate values for these weightings *a priori* is an open problem in adaptive control.

It is perhaps useful to classify the systems studied here using the notation proposed in the recent work of [24]. For our systems there is one state and two adaptive gains, therefore a 1+2 system. However, if the input (demand) signal is set to zero, one of the adaptive gains becomes redundant, and we get a 1+1 system similar to that studied by [21, 23]. The other main difference with the system studied here is that the primary system state is actually the error between two scalar linear systems.

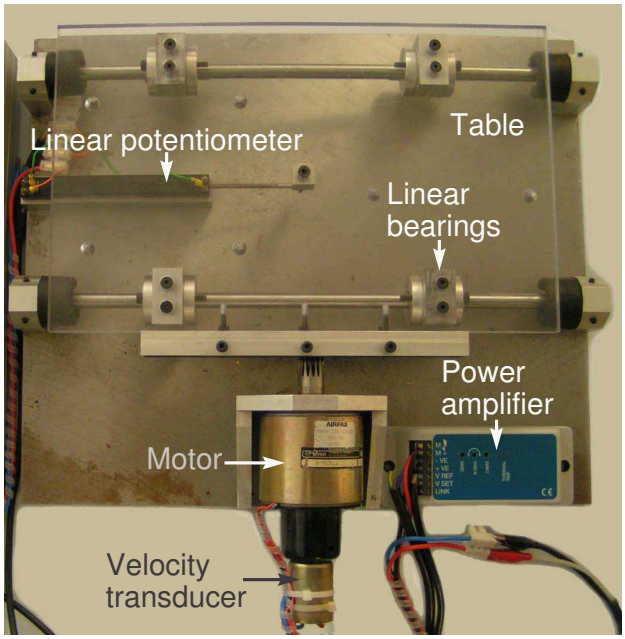

Figure 1: Photograph of the experimental plant, which is a small-scale motor-driven single axis moving table.

3 MRAC applied to a nonsmooth plant

MRAC controllers are designed to adapt to compensate for plant under-modeling and non-linearities. However it is well known that they are susceptible to gain wind-up due to noise and other uncertainties [14,25] which can lead to system instability. In this section the application of MRAC to the control of a motor rig which contains a significant deadzone nonsmooth effect is considered. This typically leads to gain wind-up — discussed in Section 3.1. In Section 3.2 a localized stability analysis for the *smooth* system is presented which demonstrates the mechanism behind wind-up.

3.1 Gain wind-up

In this paper, the plant considered is a small-scale motor-driven moving table. The plant is shown in Figure 1. The control signal, u, is generated in dSpace, a digital signal processor based system which is programmable from within the Matlab-Simulink environment. This signal is fed to the motor via a four-quadrant power amplifier. The angular velocity of the motor may be measured using a small generator (which, at low frequency, has negligible dynamics relative to those of the motor) and is calibrated to act as a tachometer. The Perspex table, which is mounted on linear bearings, is driven by the motor through a rack and pinion and the displacement

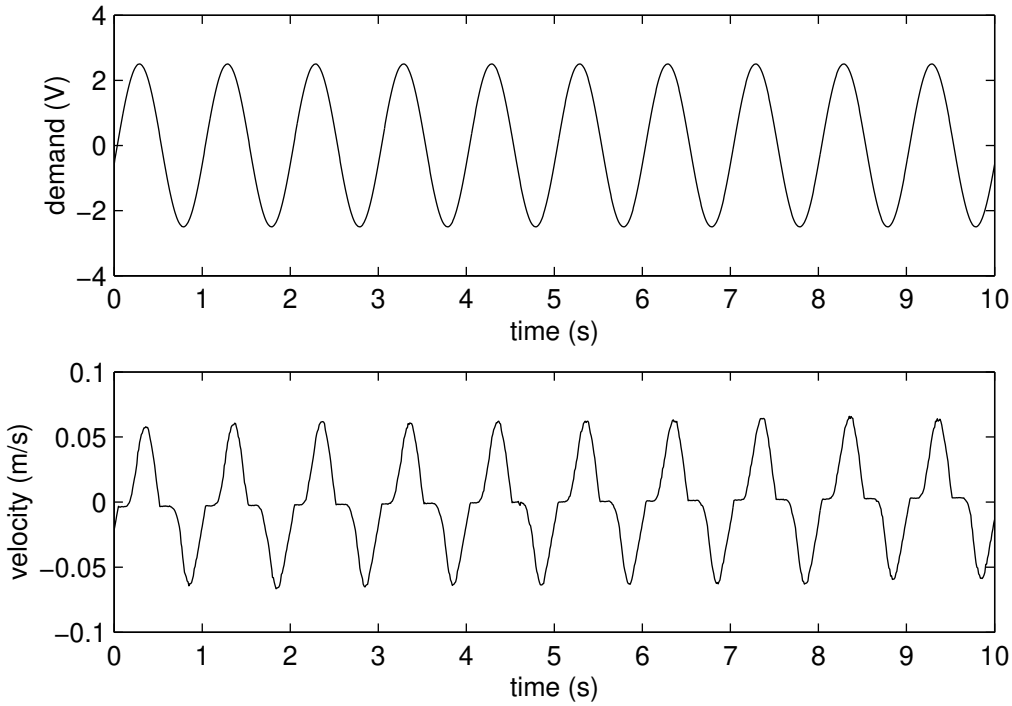

Figure 2: Experimental results showing the velocity deadzone behavior exhibited by the plant; (a) open-loop demand and (b) velocity response.

of the table is measured using a linear potentiometer.

At low frequencies the velocity of the plant exhibits behaviour which closely replicates a deadzone nonlinearity. Where, theoretically, an ideal deadzone nonlinearity is defined as:

$$\begin{aligned} v_o &= 0 \qquad \text{for} \quad |v_i| < v_c, \\ v_o &= v_i - v_c \quad \text{for} \quad v_i \geq v_c, \\ v_o &= v_i + v_c \quad \text{for} \quad v_i \leq -v_c, \end{aligned} \tag{10}$$

where v_i is the input, v_o is the output and v_c is the deadzone offset. Experimentally, the deadzone behaviour is demonstrated in Figure 2, for the case where a sinusoidal, 1Hz, 2.5V amplitude, open-loop input (Figure 2 (a)) is applied to the plant. The velocity response, Figure 2 (b), clearly exhibits regions of zero velocity lasting around 0.1s every time the direction of travel changes, which may be approximated as a deadzone nonlinearity. For this plant, it is thought that the deadzone is caused by a combination of the power amplifier dynamics and stiction in the motor and linear bearing.

A first-order MRAC strategy is used to control the displacement of the moving table. It is worth noting that in the case of a plant with a velocity deadzone, velocity control using MRAC strategies do not greatly assist

with the minimization of the nonlinear plant behavior. This is because with velocity control the magnitude of both the demand velocity, r, and the feedback velocity, x, are small, assuming that (as would normally be the case) the demand frequency is lower than the reference model break frequency. Therefore the rate of change in the controller gains are small over the region where non-linear behavior occurs. Conversely, with displacement control, the non-linear regions coincide with the regions of large amplitude displacements x and r and therefore rapid gain adaption can occur over the non-linear regions, giving more responsive control.

Figures 3 (a) and (b) show the plant displacement x compared with the reference model output x_m and the system gains respectively when the plant displacement is controlled using the MRAC algorithm. The reference model parameters used were $a_m = b_m = 40$ and the demand was a 0.02m amplitude, 0.8Hz sinusoid. Initially the gains are set to $K_{r0} = 52$ and $K_0 = -42$ which were found to give reasonably smooth linear control. Over the first 10s of the test the adaptive gain weightings α and β were set to zero, i.e. a constant gain linear control strategy was used. It can be seen that over this period of time the table response was reasonably good except over the non-linear velocity deadzone regions where there is a marked error between the table displacement and the reference model output. At $t = 10$s the unmodified adaptive MRAC strategy was activated by setting non-zero adaptive gain weightings ($\alpha = 10$ and $\beta = 1$). It can be seen that with the adaptive control strategy the gains rapidly changed (in this case winding down) resulting in very poor displacement control, and within 6 oscillations at 18.5s the maximum positive travel of the table was exceeded. This type of stability loss was observed with lower adaptive gain weightings over an extended time frame and has been observed in other nonsmooth systems [11]. The mechanism behind this type of stability loss is considered next.

3.2 Localized analysis of the MRAC algorithm

In this section the error equation (Equation (7)) developed in Section 2 is reformulated as a nonlinear dynamical system. Using a dynamical systems approach the system stability can be analyzed using local analysis close to the equilibrium points. The plant and MRAC algorithm is assumed to be a dynamical system of the form

$$\dot{\xi} = f(\xi, t), \tag{11}$$

where $\xi = \{x_e, K, K_r\}^T$ is the state vector.

By manipulating Equation (7) and the derivatives of Equations (8) and (9), the dynamical system repre-

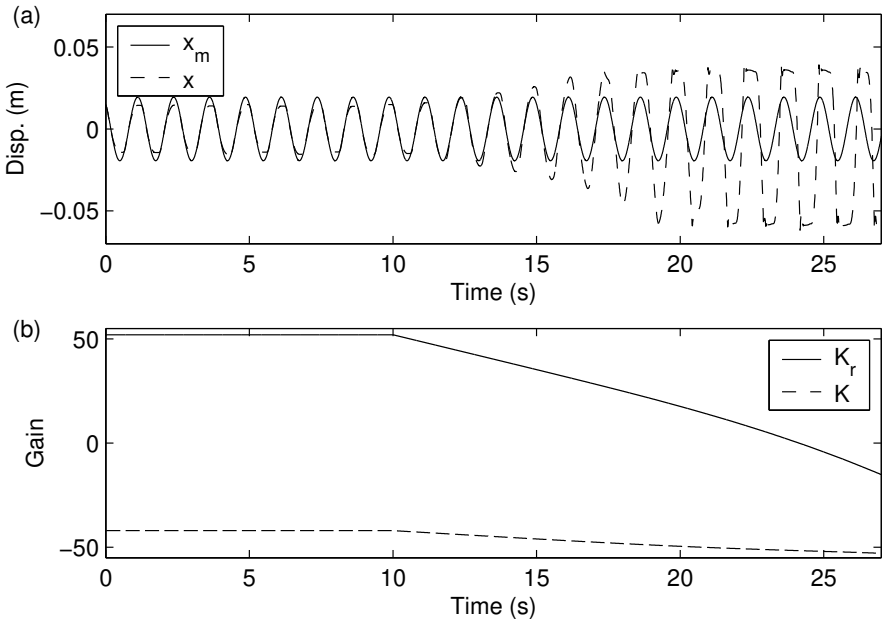

Figure 3: Displacement control of the experimental plant using the standard unmodified MRAC algorithm, initially using linear gains ($\alpha = \beta = 0$) with adaptive gain weighting set to $\alpha = 10$, $\beta = 1$ at $t = 10$s; (a) displacement response and (b) system gains.

sentation of the plant and MRAC algorithm may be expressed as

$$\begin{aligned}
\dot{x}_e &= -a_m x_e + b\left(K^E - K\right)(x_m - x_e) + b\left(K_r^E - K_r\right) r \\
\dot{K} &= \alpha\left(x_e x_m - x_e^2\right) + \beta\left\{x_e \dot{x}_m + (x_m - 2x_e)\left[-a_m x_e + b\left(K^E - K\right)(x_m - x_e) + b\left(K_r^E - K_r\right) r\right]\right\} \\
\dot{K}_r &= \alpha x_e r + \beta\left\{x_e \dot{r} + r\left[-a_m x_e + b\left(K^E - K\right)(x_m - x_e) + b\left(K_r^E - K_r\right) r\right]\right\},
\end{aligned} \tag{12}$$

where the parameters a_m, b, α and β are constant and the parameters r, $\dot{r}$, x_m and $\dot{x}_m$ are time varying input signals (see Appendix A1 for a formulation using the variables $(K^E - K)$ and $(K_r^E - K_r)$ in place of K and K_r).

The first step is to find the equilibrium points of Equation (12). Having done this the stability of each equilibrium point can be examined using local analysis of the linearized system. To find the equilibrium points for the system we need to solve the equation: $f(\tilde{\xi}, t) = 0$, where ($\tilde{}$) indicates an equilibrium point. By inspection, two conditions are necessary for the system to be at equilibrium

$$\tilde{x}_e = 0, \tag{13}$$

$$(K^E - \tilde{K})x_m + (K_r^E - \tilde{K}_r)r = 0, \tag{14}$$

from which it can be seen that there are an infinite number of $\tilde{K}$, and corresponding $\tilde{K}_r$, values which give $f(\tilde{\xi}, t) = 0$.

Defining a subset of the complete system state space as $\Sigma = \{x_e \times K \times K_r \in \mathbb{R}^3\}$, then Equations (13) and (14) define the equilibrium manifold (denoted Γ) which represents the set of equilibrium points $\tilde{\xi} = \{0, \tilde{K}, \tilde{K}_r\}^T$. In the case of $\dot{r} = \dot{x}_m = 0$ and x_m/r constant (this is the case for a steady state unit step input) the manifold representing the equilibrium solutions in Σ defined by Equation (14) is a straight line in the K, K_r plane. The projection of the dynamics onto Γ for the step input case is shown in Appendix A2.

In general, however, r and x_m are time varying (with the relationship between x_m and r being governed by Equation (3). Equation (14) will be satisfied regardless of x_m and r if $\tilde{K} = K^E$ and $\tilde{K}_r = K_r^E$ corresponding to the equilibrium point at $\hat{\xi}_E = \{0, K^E, K_r^E\}^T$. In addition to this time invariant point, there are an infinite number of time dependent solutions to Equation (14) which require time varying $\tilde{K}$ and $\tilde{K}_r$ for time varying x_m and r. However, from Equations (12) it can be observed that for $\tilde{K}$ and $\tilde{K}_r$ to vary with time the error x_e must be non-zero. Therefore at equilibrium points other than $\tilde{\xi}_E = \{0, K^E, K_r^E\}^T$, limit cycle type behavior exists which oscillate around Γ. The existence of oscillations in the gain can also indicate factors such as under-modeling of the plant.

To analyze the local stability of the system near an equilibrium points $\tilde{\xi}$, the right hand side of Equation (11) is expanded as a Taylor series at $\tilde{\xi}$, from which the linear approximation to the system is

$$\dot{\xi} \approx Df_\xi(\hat{\xi})(\xi - \hat{\xi}), \tag{15}$$

where $Df_\xi(\hat{\xi})$ is the Jacobian Matrix evaluated at an equilibrium point $\xi = \hat{\xi}$, $f(\tilde{\xi}) = 0$, and all the $\mathcal{O}((\xi - \tilde{\xi})^2)$ and higher terms have been neglected. The stability of the local dynamics is given by the eigenvalues of $Df_\xi(\tilde{\xi})$. Using Equation (12), the Jacobian for the system at an equilibrium point $\tilde{\xi}$ is found to be

$$Df_\xi(\tilde{\xi}) = \begin{bmatrix} -a_m - b(K^E - \tilde{K}) & -bx_m & -br \\ \alpha x_m - \beta[a_m x_m + b(K^E - \tilde{K})x_m - \dot{x}_m] & -\beta b x_m^2 & -\beta b r x_m \\ \alpha r - \beta[a_m r + b(K^E - \tilde{K})r - \dot{r}] & -\beta b x_m r & -\beta b r^2 \end{bmatrix}. \tag{16}$$

This Jacobian has three eigenvalues, $\lambda_1 = 0$ and

$$\lambda_{2,3} = -\frac{1}{2}[a_m + b(K^E - \tilde{K}) + \beta b(x_m^2 + r^2)] \pm \frac{1}{2}S, \tag{17}$$

where $S^2 = [a_m + b(K^E - \tilde{K}) + \beta b(x_m^2 + r^2)]^2 - 4b[\alpha(x_m^2 + r^2) + \beta(x_m\dot{x}_m + r\dot{r})]$. It should emphasized at this point that λ_1 is time invariant, and indicates neutral (i.e. non-asymptotic) stability in the eigenvector direction which is given by

$$e_1 = [0, -r/x_m, 1]^T. \tag{18}$$

In this case the eigenvector, e_1 is always tangent to the exact matching manifold, Γ.

Figure 4 (a) shows the adaptive gains for a simulation of first-order plant controlled using the unmodified MRAC strategy. The initial gains were set to zero, and the adaptive weightings where $\alpha = 1000$ and $\beta = 100$. The plant and reference model parameters used were $a = b = 4$ and $a_m = b_m = 40$ respectively and the demand r was a 1V amplitude 1Hz sinusoid. It can be seen that the gains settle to the Erzberger values of $K^E = -9$ and $K_r^E = 10$ in around 20 seconds. However if noise disturbance is added to the plant output, gain wind-up can occur as shown in Figure 4 (b), where a 50Hz 0.1V sinusoid is added to the plant output. Yang [25] shows that the neutral localized stability in the direction of the equilibrium manifold leads to gain wind-up when a system is subjected to noise and that the wind-up occurs along the manifold (Γ) i.e. in the direction of $\pm e_1$, depending on system parameters and input signals.

4 The modified MRAC algorithm

To alleviate the problem of gain wind-up, a method is presented for replacing the undesirable zero eigenvalue with a constant (real) negative eigenvalue. This is achieved by replacing the time varying adaptive gains K and K_r with new modified gains, K_m and K_{rm} respectively, resulting in the control equation

$$u(t) = K_m(t)x(t) + K_{rm}(t)r(t) \tag{19}$$

The modified gains are calculated using the equations

$$K_m = \frac{s}{s + \rho^2}K + \frac{\rho^2}{s + \rho^2}K^* \tag{20}$$

$$K_{rm} = \frac{s}{s + \rho^2}K_r + \frac{\rho^2}{s + \rho^2}K_r^* \tag{21}$$

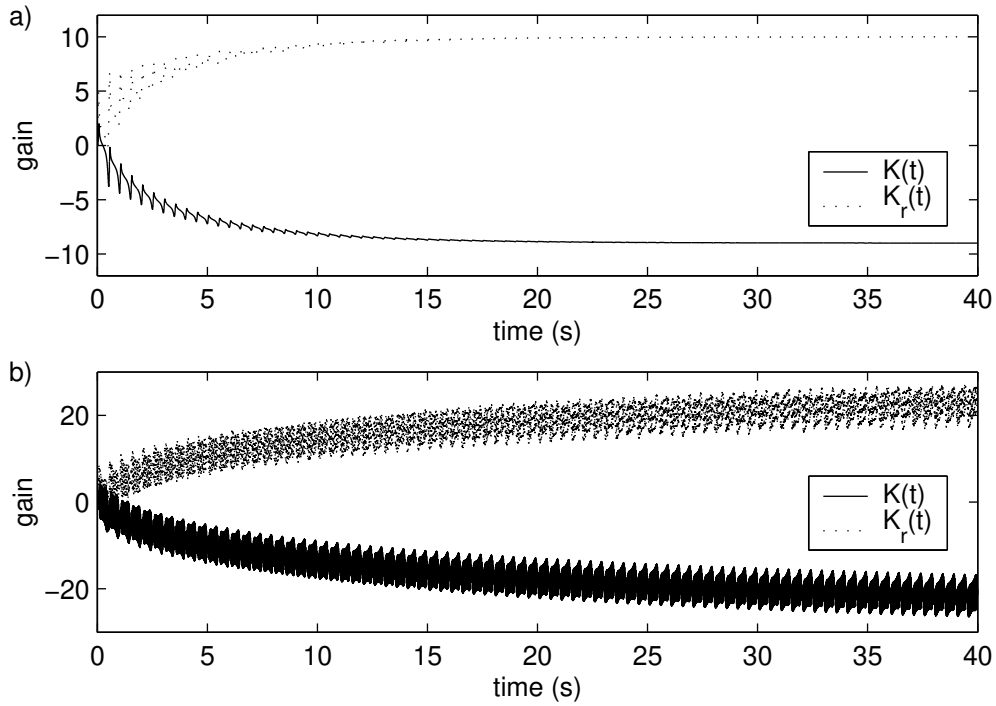

Figure 4: Simulation of a plant controlled using the MRAC algorithm, a) with no noise and b) with noise added to the plant output, using plant parameters $a = b = 4$ and reference model parameters $a_m = b_m = 40$.

where s is the Laplace transform variable, ρ is a constant and K^* and K_r^* are gain constants. A condition on the values of these gain constants is derived in the subsequent analysis. Similar gain "leakage" strategies, have been applied to an integral only adaptive gain strategy, i.e. a MRAC controller with $\beta = 0$ — these are discussed in [14]. It can be seen from equations 20 and 21 that the modified gains K_m and K_{rm} are generated using two signals filtered by first-order transfer functions - a high-pass first-order filter applied to K or K_r respectively and a low-pass first-order filter applied to K^* or K_r^* respectively.

4.1 Dynamics of the modified algorithm

By considering the localized stability of the modified system it can be shown that all three system eigenvalues are stable. The error dynamics for the modified system may be expressed as

$$\begin{aligned}
\dot{x}_e &= -a_m x_e + b\left(K^E - K_m\right)(x_m - x_e) + b\left(K_r^E - K_{rm}\right) r \\
\dot{K}_m &= \alpha\left(x_e x_m - x_e^2\right) + \beta\left\{x_e \dot{x}_m + (x_m - 2x_e)\left[-a_m x_e + b\left(K^E - K_m\right)(x_m - x_e) + b\left(K_r^E - K_{rm}\right) r\right]\right\} \\
&\quad +\rho^2(K^* - K_m) \\
\dot{K}_{rm} &= \alpha x_e r + \beta\left\{x_e \dot{r} + r\left[-a_m x_e + b\left(K^E - K_m\right)(x_m - x_e) + b\left(K_r^E - K_{rm}\right) r\right]\right\} + \rho^2(K_r^* - K_{rm}),
\end{aligned} \tag{22}$$

By inspection, there are now four conditions that are necessary for the system to be at equilibrium:

$$\tilde{x}_e = 0 \tag{23}$$

$$(K^E - \tilde{K}_m)x_m + (K_r^E - \tilde{K}_{rm})r = 0 \tag{24}$$

$$\tilde{K}_m = K^* \tag{25}$$

$$\tilde{K}_{rm} = K_r^* \tag{26}$$

Note that if $\rho = 0$ we revert to the unmodified case where only the first two conditions are required.

For these four conditions (23)–(26) to be satisfied it follows that, since x_m and r are time varying, $K^* = K^E$ and $K_r^* = K_r^E$ and that equilibrium only exists at a single point, $\tilde{\xi}_E = \{0, K^E, K_r^E\}^T$. In Section 3 it was shown that with the standard MRAC strategy there exists a manifold of equilibrium points (Γ), and that the Jacobian of each equilibrium point had a zero eigenvalue. For the modified algorithm the manifold of equilibrium points has been reduced to a single point, and computing the Jacobian matrix reveals that the time invariant eigenvalue now takes the value $\lambda_1 = -\rho^2$ in the eigenvector direction $e_1 = [0, -r/x_m, 1]^T$.

Therefore the modification to the MRAC algorithm has eliminated the neutral (i.e. non-asymptotic) localized stability. However, to implement the controller, knowledge on the Erzberger gains are needed to select K^* and K_r^*. In practice these gain values will not be known accurately but can be estimated from a first-order transfer function approximation to the plant dynamics. Errors in the estimation of the Erzberger gains used for setting K^* and K_r^* will cause oscillations in the gains about the K^* and K_r^* values. This is demonstrated in simulation in Figure 5 (a) where $K^* = -10$ and $K_r^* = 12$ (the Erzberger gains are $K^E = -9$ and $K_r^E = 10$) and $\rho = 2$ with the other parameters taking the values used in Figure 4. With the addition of the noise on the

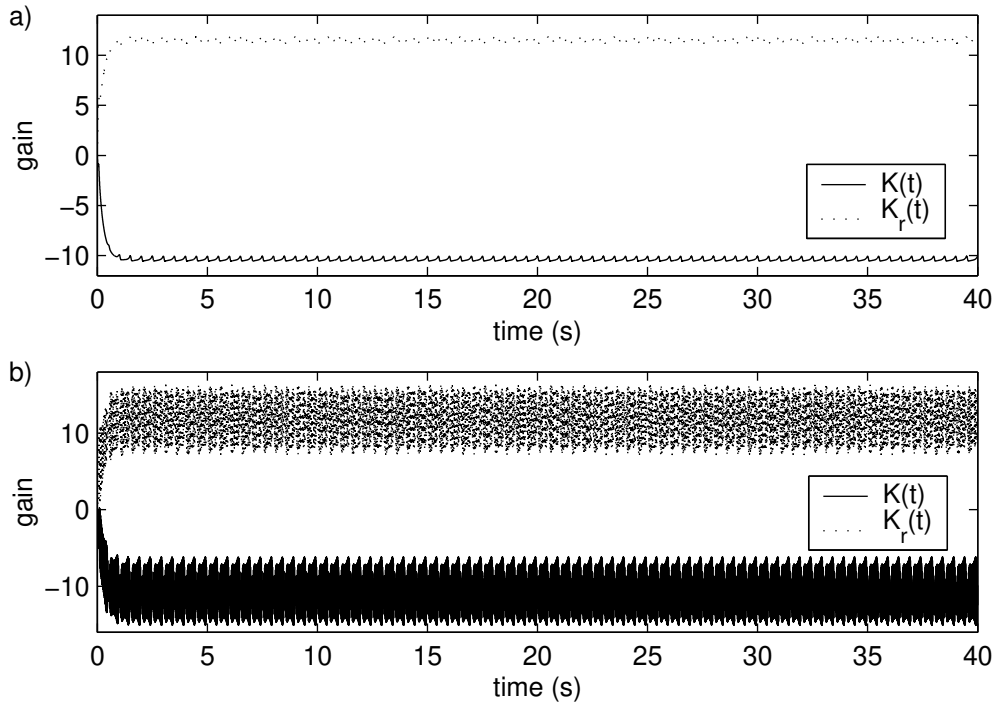

Figure 5: Simulation of a plant controlled using the modified MRAC algorithm, a) with no noise and b) with noise added to the plant output, using plant parameters $a = b = 4$ and reference model parameters $a_m = b_m = 40$. Note the gain oscillations which occur in (a) are due to $K^* \neq K^E$ and $K_r^* \neq K_r^E$.

plant output, Figure 5 (b), it can be seen that the modified control algorithm has eliminated the gain wind-up.

One possible method for overcoming the need for setting K^* and K_r^* values based on estimates of the Erzberger gains is to start controlling the plant using the standard MRAC algorithm (i.e. $\rho = 0$). Then as the gains adapt, the modification could be activated, at say $t = t_\rho$, by setting a non-zero ρ value and setting K^* and K_r^* values to the current gain values, $K(t_\rho)$ and $K_r(t_\rho)$ respectively. However, for the plant considered in this paper the standard MRAC algorithm was insufficiently stable for this method to be practical. Instead the K^* and K_r^* gains were set to the gain values that were found to provide good linear (fixed-gain) control, $K_r = 52$ and $K = -42$.

4.2 Experimental implementation

For the moving table, it has already been shown, in Figure 3 that when the standard MRAC strategy is used gain wind-up occurs which leads to system instability. Using the modified algorithm, Figures 6 (a), (b) and (c) show the displacement response and the system gains K_r and K respectively for the case where $\rho = 10$, $\alpha = 2000$, $\beta = 200$, $K_r^* = 52$ and $K^* = -42$. The traces are shown after 40s of adaption, and it can be seen that with this modified MRAC strategy the control is significantly better than the linear control shown in the first 10s of Figure 3. In this case there is only a limited deterioration of the control accuracy over the velocity deadzone regions. Note also that the unmodified MRAC approach, shown after 10s in Figure 3, could not control this plant at all.

Figures 6 (b) and (c) show how the gains adapt in a regular oscillatory pattern at twice the frequency of the demand. It is interesting to note that the gains also exhibit a very slight gain wind-up. The analysis in the previous section suggested that with the modified algorithm no gain wind-up would occur. However, this analysis was based on the dynamics of the plant being approximated to a first-order linear system. There are two contributing factors for the small amount of gain wind-up observed in the experiments; (i) The gains have not yet fully adapted to the final values. Simulations of the modified algorithm indicate that if $K^* \neq K^E$ and $K_r^* \neq K_r^E$ that there is a very slow movement of trajectories in Σ towards the single fixed point, $\tilde{\xi}_E$. (ii) There is significant under-modeling of the plant dynamics. In this case the plant dynamics may be more accurately modelled as second order than as first order. Also the nonsmooth discontinuity in the plant is not included in the analysis of section 3.2.

We have used a modified version of the MRAC algorithm to successfully control a plant with a nonlinear deadzone. To assess the effectiveness of such a controller it is worth examining the control of the plant when using the linear equivalent to the MRAC algorithm, i.e. the MRAC controller with adaptive weightings α and β set to zero. Figures 7 (a) and (b) show comparisons of the table performance using the modified MRAC algorithm and the linear equivalent to the adaptive MRAC strategy. The fixed gains in the linear controller take the same values as the modified MRAC K_r^* and K^* gains. Figure 7 (a) shows the displacement response using the linear and the adaptive modified MRAC controllers compared to the reference model displacement x_m. It can be seen that the performance of the modified MRAC strategy is better than that of the linear control equivalent, especially over the non-linear deadzone regions. The errors, $x_m - x$ for the two control

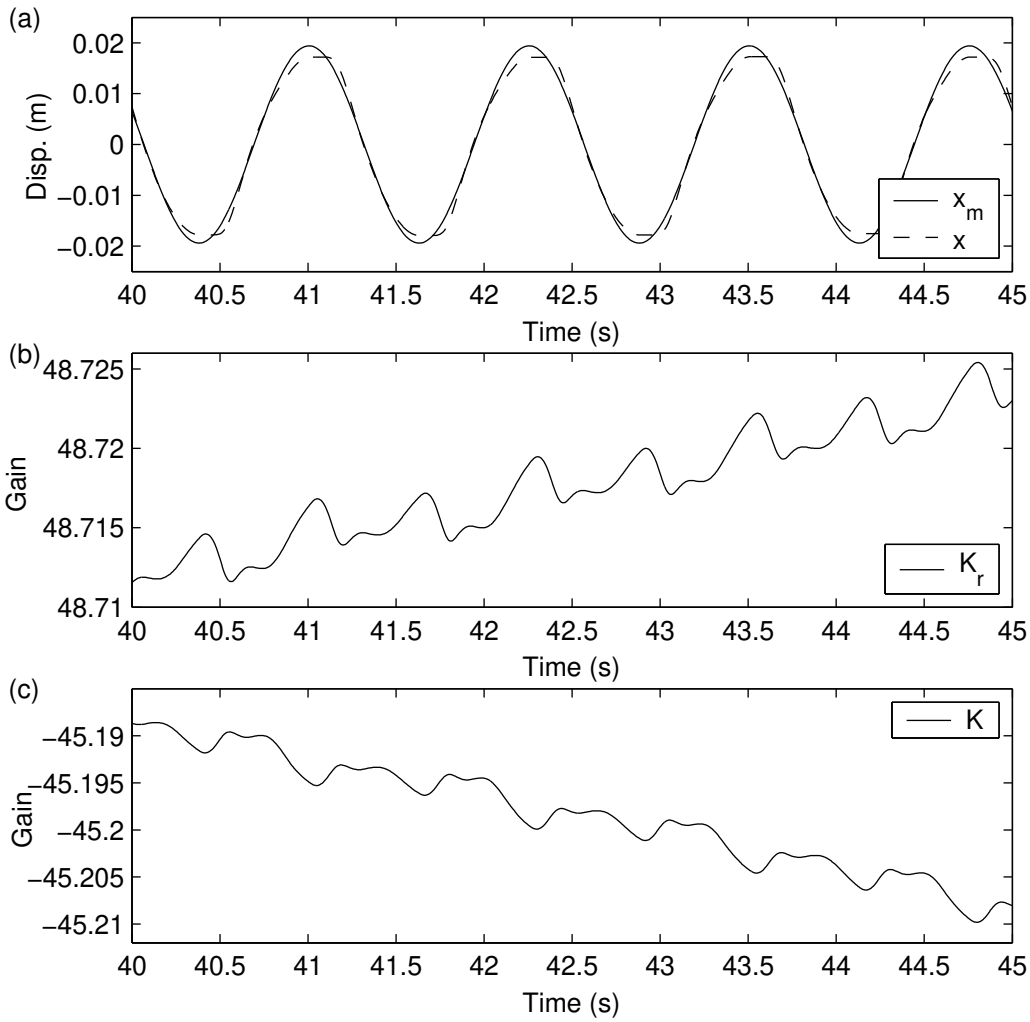

Figure 6: Experimental results showing displacement control of the plant using the modified MRAC algorithm; (a) displacement response, (b) and (c) system gains.

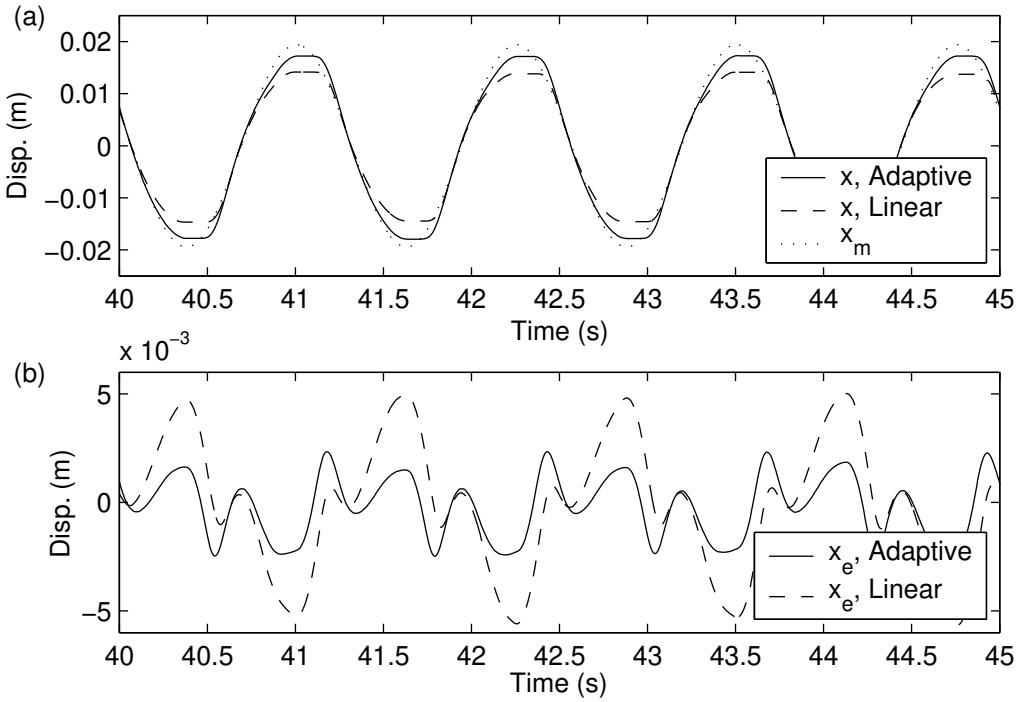

Figure 7: Experimental results showing displacement control of the plant using the linear equivalent to the MRAC algorithm; (a) displacement response and (b) system error $x_m - x$.

strategies are shown in Figure 7 (b), where the modified adaptive error is approximately half the maximum amplitude of that of the linear control.

5 Conclusions

In this paper a modified MRAC controller has been presented which has been applied to a nonsmooth plant. The phenomena of gain wind-up, which commonly occurs in MRAC control systems, has been analyzed using localized stability analysis. Using this analysis the inherent zero eigenvalue which exists in the unmodified system, is seen to be the major cause of gain wind-up in the presence of plant uncertainties such as a nonsmooth discontinuities. A modification to the MRAC strategy has been proposed to eliminate the zero eigenvalue and reduce the infinite manifold of equilibrium solutions, Γ, to a single equilibrium point, $\tilde{\xi}_E$. Simulations of a plant with first order dynamics have been used to demonstrate the presence of gain wind-up when the plant output is subjected to a noise disturbance in the unmodified MRAC. However, with the modification to the control strategy, the simulations demonstrate that gain wind-up does not occur.

Experimental testing of the MRAC strategy was performed on a small-scale motor-driven moving table in displacement control. The table dynamics are nonsmooth, with the velocity response exhibiting a large dead-zone nonlinearity. Initially tests were conducted on a linear equivalent to the MRAC strategy (i.e. equivalent to setting the MRAC adaptive gain weightings to zero). With tuning, the linear controller performed reasonably well. However when the gains were allowed to adapt, using the standard unmodified MRAC strategy, the control performance was very poor, to the extent that it was impossible to get the unmodified MRAC to stabilize. The control of the table using the modified MRAC strategy was a significant improvement both on the linear control and the unmodified MRAC. The modified MRAC, had approximately half the maximum displacement error than when the linear controller was used. The gains oscillations observed in the experimental results occurred at twice the frequency of the demand signal with a slight gain wind-up. This wind-up can be attributed to continued gain evolution at a slow rate and under-modeling of the plant dynamics.

In the future, it is anticipated that further refinement of the modified MRAC algorithm will be possible. In particular, it would be beneficial for K^* and K_r^* to be optimised on-line to minimise the oscillations in K_m and K_{rm}, as was observed in the simulation results due to errors in matching K^* and K_r^* to K^E and K_r^E respectively. In addition to this, a systematic technique for selecting the optimal value of rho for a particular plant would be a highly desirable research objective. The improvement in robustness which can be achieved by the modifications demonstrated in this work may also lead to this type of algorithm being applicable to a wider range of practical applications.

6 Acknowledgements

Lin Yang would like to acknowledge the support of the Dorothy Hodgkin Postgraduate Award scheme. The authors would also like to acknowledge the support of the EPSRC. David Virden is supported by research grant GR/R99539/01 and David Wagg by an Advanced Research Fellowship.

Appendix

In appendix A1 we outline the background material on the derivation of MRAC for systems of higher order which would naturally be written in a matrix formulation. In appendix A2 we describe how expressions can

be obtained for the global dynamics along Γ.

A1 Higher-order MRAC formulations

For the linear state space system in the form $\dot{x}(t) = Ax(t) + Bu(t)$, where x is the $n \times 1$ state variable vector, u is the $m \times 1$ control signal vector, A is a $n \times n$ matrix representing the linear dynamics of the plant, and B is a $n \times m$ matrix. The controller is given by $u(t) = K(t)x(t) + K_r(t)r(t)$, where $r(t)$ is the reference (demand) signal, $K(t)$ is the feedback adaptive gain and $K_r(t)$ the feed forward adaptive gain [13–15]. All the input signals we use in this work are at least persistently exciting to order one [14]. Substituting for u gives

$$\dot{x} = Ax + B(Kx + K_r r) = (A + BK)x + BK_r r. \tag{27}$$

The plant is now controlled to follow the output from a reference model with known dynamics $\dot{x}_m(t) = A_m x_m(t) + B_m r(t)$, where x_m is the state of the reference model and A_m and B_m are linear reference equivalents of A and B [12]. The system error dynamics are now

$$\dot{x}_e = A_m x_e + (A_m - A - BK)x + (B_m - BK_r)r, \tag{28}$$

and for exact matching $A + BK^E = A_m$ and $BK_r^E = B_m$. Assuming all matrix (pseudo) inverses exist we can obtain expressions (the Erzberger conditions [15]) for the gain values as $K^E = B^\dagger(A_m - A)$ and $K_r^E = B^\dagger B_m$, where $()^\dagger$ denotes the pseudo-inverse and $()^E$ denotes the constant Erzberger gain value. The Erzberger gains can be used to express the matrix terms given in Equation (28), as

$$\dot{x}_e = A_m x_e + B\Phi^T w \tag{29}$$

where $\Phi = (K^E - k)$, $k = \{K, K_r\}^T$,$K^E = \{K^E, K_r^E\}^T$ and $w(t) = \{x, r\}^T$ and we assume that B has a pseudo-inverse such that $BB^\dagger = I$. The adaptive gains are defined in a proportional plus integral formulation

$$k = \alpha \int_0^t y_e w(\tau) \mathrm{d}\tau + \beta y_e w(t). \tag{30}$$

where α and β are control weightings representing the adaptive effort, and $y_e = C_e x_e$ where C_e can be chosen to ensure the stability of the feed forward block [12].

If we let $\phi(t) = (K^E - K(t))$ and $\psi(t) = (K_r^E - K_r(t))$, then $\Phi(t) = \{\phi, \psi\}^T$ and $\xi = \{x_e, \phi, \psi\}^T$ is the state vector. By using the fact the K^E is a constant, $\dot{\Phi} = -\dot{k}$, and by using Equation (30) we can obtain expressions for $\dot{\phi}$ and $\dot{\psi}$.

Applying this formulation to the first order plant/controller system described in 2 gives the following system of ODE's (assuming C_e is incorporated into α and β)

$$\begin{aligned}
\dot{x}_e &= -a_m x_e + b[\phi(x_m - x_e) + \psi r], \\
\dot{\phi} &= -\alpha x_e(x_m - x_e) - \beta[(-a_m x_e + b[\phi(x_m - x_e) + \psi r])(x_m - 2x_e) + x_e \dot{x}_m], \\
\dot{\psi} &= -\alpha x_e r - \beta((-a_m x_e + b[\phi(x_m - x_e) + \psi r])r + x_e \dot{r}).
\end{aligned} \tag{31}$$

In this formulation $\tilde{\xi}_E = \{0, 0, 0\}$.

A2 Global dynamics along Γ

Using Equation (31) we can define a subset of the complete state space $\hat{\Sigma} = \{\mathbb{R} \times \mathbb{R} \times \mathbb{R} : (x_e, \phi, \psi)\}$. Then by defining a transformation matrix $T = [e_1, e_2, e_3]$, consisting of the eigenvectors of the linearized system, the transformation $\xi = T\nu$ can be made where $\nu = [u, v, w]$. Rewriting Equation (31) in the form $\dot{\xi} = L\xi + h(\xi)$, where L is the linear part and $h(\xi)$ the nonlinear part, gives an expression for the dynamics in the transformed coordinates

$$\begin{bmatrix} \dot{u} \\ \dot{v} \\ \dot{w} \end{bmatrix} = T^{-1}LT \begin{bmatrix} u \\ v \\ w \end{bmatrix} + T^{-1}h(\xi). \tag{32}$$

In this coordinate set, $\dot{u}$ represents the dynamics along the exact matching manifold, Γ, and $T^{-1}LT$ has the following block diagonal structure

$$T^{-1}LT = \begin{bmatrix} 0 & \vdots & 0 & 0 \\ \cdots & \cdots & \cdots & \cdots \\ 0 & \vdots & s_{12} & s_{12} \\ 0 & \vdots & s_{21} & s_{22} \end{bmatrix} \tag{33}$$

where s_{ij} represents an unspecified algebraic term. Now $T^{-1}LT$ is in a block diagonal form as discussed by [20] in relation to center manifolds. In effect the dynamics associated with the zero eigenvalue — the leading diagonal term in $T^{-1}LT$ — have been linearly decoupled from the dynamics associated with the stable eigenvalues — represented by the block formed by the s_{ij}, $i, j = 1, 2$ terms. However, unlike the classical approach to center manifold theory for the systems described by [20, 29], the adaptive system has a time invariant zero eigenvalue. The result is that the dynamics associated with the zero eigenvalue can be projected

onto Γ, and for a step input, Γ is a linear time invariant manifold. Therefore Γ is the center manifold in the system. A similar type of center manifold analysis has been carried out for a different class of adaptive systems by [21]. As pointed out by [21], decoupling the center manifold dynamics allows us to ignore the remaining system dynamics.

The dynamics along Γ can be extracted from Equation (32) as the first row of T^{-1} multiplied by the nonlinear vector $h(\nu)$.

$$\dot{u} = [T_{11}^{-1}, T_{12}^{-1}, T_{13}^{-1}] \begin{bmatrix} h_1(\xi) \\ h_2(\xi) \\ h_3(\xi) \end{bmatrix} \tag{34}$$

The form of Equation (34) will then enable us to determine the dynamics along Γ. For the step input case, the matrix of linear terms is

$$L = \begin{bmatrix} -a_m & b & b \\ -\alpha + \beta a_m & -\beta b & -\beta b \\ -\alpha + \beta a_m & -\beta b & -\beta b \end{bmatrix} \tag{35}$$

and the nonlinear vector

$$h(\xi) = \begin{bmatrix} -b\phi x_e \\ -\alpha x_e^2 - \beta[2a_m x_e^2 - 3b\phi x_e + 2b\phi x_e^2 - 2b\psi x_e] \\ \beta b\phi x_e \end{bmatrix} \tag{36}$$

The transformation matrix, T has the form

$$T = \begin{bmatrix} 0 & \hat{\lambda}_2/\chi & \hat{\lambda}_3/\chi \\ -1 & 1 & 1 \\ 1 & 1 & 1 \end{bmatrix} \tag{37}$$

where $\hat{\lambda}_i = \lambda_i + 4\beta b$, $i = 1, 2$ and $\chi = (\beta a_m + b\tilde{\phi}\beta - \alpha)$. The inverse transform matrix is then given by

$$T^{-1} = \begin{bmatrix} 0 & \frac{1}{2} & -\frac{1}{2} \\ -\frac{\chi}{\hat{\lambda}_3 - \hat{\lambda}_2} & \frac{1}{2}\frac{\hat{\lambda}_3}{\hat{\lambda}_3 - \hat{\lambda}_2} & \frac{1}{2}\frac{\hat{\lambda}_3}{\hat{\lambda}_3 - \hat{\lambda}_2} \\ \frac{\chi}{\hat{\lambda}_3 - \hat{\lambda}_2} & -\frac{1}{2}\frac{\hat{\lambda}_2}{\hat{\lambda}_3 - \hat{\lambda}_2} & -\frac{1}{2}\frac{\hat{\lambda}_2}{\hat{\lambda}_3 - \hat{\lambda}_2} \end{bmatrix} \tag{38}$$

such that

$$\dot{u} = \frac{1}{2}h_2(\xi) - \frac{1}{2}h_3(\xi) \tag{39}$$

substituting for h gives

$$\dot{u} = \beta b(\phi + \psi)x_e - (\frac{\alpha}{2} + \beta(a_m + b\phi))x_e^2. \tag{40}$$

Then from the relation $\xi = T\nu$

$$\begin{aligned} x_e &= \tfrac{\lambda_2}{\chi}v + \tfrac{\lambda_3}{\chi}w \\ \phi &= -u + v + w \\ \psi &= u + v + w \end{aligned} \tag{41}$$

so that we can obtain an expression for the dynamics along Γ in terms of the coordinate set ν,

$$\dot{u} = 2\beta b(v + w)(\frac{\hat{\lambda}_2}{\chi}v + \frac{\hat{\lambda}_3}{\chi}w) - (\frac{\alpha}{2} + \beta(a_m + b(-u + v + w)))(\frac{\hat{\lambda}_2}{\chi}v + \frac{\hat{\lambda}_3}{\chi}w)^2. \tag{42}$$

From equation (40) , if $x_e \neq 0$ then $\dot{u}$ will have some value which represents the rate of change of the coordinate along (i.e. tangent to) the exact matching manifold, Γ.

References

[1] Qammar, H. K., and Mossayebi, F., 'System identification and model based control of a chaotic system', *International Journal of Bifurcation and Chaos* **4(4)**, 1994, 843–851.

[2] Petrov, V., Crowley, M. F., and Showalter, K., 'An adaptive control algorithm for tracking unstable periodic orbits', *International Journal of Bifurcation and Chaos* **4(5)**, 1994, 1311–1317.

[3] Wu, C. W., Yang, T., and Chua, L. O., 'On adaptive synchronization and control of nonlinear dynamical systems', *International Journal of Bifurcation and Chaos* **6(3)**, 1996, 455–471.

[4] Stoten, D. P., and Di Bernardo, M., 'Application of the minimal control synthesis algorithm to the control and synchronization of chaotic systems', *International Journal of Control* **65(6)**, 1996, 925–938.

[5] Dong, X., Chen, G., and Chen, L., 'Adaptive control of the uncertain duffing oscillator', *International Journal of Bifurcation and Chaos* **7(7)**, 1997, 1651–1658.

[6] Di Bernardo, M., 'An adaptive approach to the control and synchronization of continuous-time chaotic systems'. *International Journal of Bifurcation and Chaos* **6(3)**, 1996, 557–568.

[7] Di Bernardo, M., *Adaptive control and analysis of nonlinear chaotic dynamical systems*, PhD thesis, University of Bristol, 1998.

[8] Wagg, D. J,. 'Adaptive control of nonlinear dynamical systems using a model reference approach'. *Meccanica* **38**, 2003, 227–238.

[9] de la Sen, M., 'Lyapunov stability and adaptive regulation of a class of nonlinear nonautonomous second-order differential equations', *Nonlinear Dynamics* **28**, 2002, 261–272.

[10] Ioannou, P. A., and Kokotovic, P. V., 'Instability analysis and improvement of robustness of adaptive control', *Automatica* **20(5)**, 1984, 583–594.

[11] Virden, D., and Wagg, D. J., 'System identification of a mechanical system with impacts using model reference adaptive control', *Proc. IMechE. Pat I: Journal of Systems and Control Engineering* **219**, 2005, 121–132.

[12] Landau, Y. D., *Adaptive control:The model reference approach*, Marcel Dekker, New York, 1979.

[13] Sastry, S., and Bodson, M., *Adaptive control:Stability, convergence and robustness*, Prentice-Hall, New Jersey, 1989.

[14] Åström, K. J., and Wittenmark, B., *Adaptive Control*, Addison Wesley, 1995.

[15] Khalil, H. K., *Nonlinear Systems*, Macmillan, New York, 1992.

[16] Mareels, I. M. Y., and Bitmead, R. R., 'Bifurcation effects in robust adaptive control', *IEEE Transactions on Circuits and Systems* **35(7)**, 1988, 835–841.

[17] Huberman, B. A., and Lumer, E., 'Dynamics of adaptive systems', *IEEE Transactions on Circuts and Systems* **37(4)**, 1990, 547–550.

[18] Gonzalez, G. A., 'Dynamical behaviour arising in the adaptive control of the generalized logistic map', *Chaos, Solitions and Fractals* **8(9)**, 1997, 1485–1488.

[19] Townley, S., 'An example of a globally stabilizing adaptive controller with a generically destabilising parameter estimate', *IEEE Transactions on Automatic Control* **44(11)**, 1999, 2238–2241.

[20] Guckenheimer, J., and Holmes, P., *Nonlinear oscillations, dynamical systems, and bifurcations of vector fields*, Springer-Verlag, New York, 1983.

[21] Leach, J. A., Triantafillidis, S., Owens, D. H., and Townley, S., 'The dynamics of universal adaptive stabilization: computational and analytical studies', *Control-Theory and Advanced Technology* **10(4)**, 1995, 1689–1716.

[22] Gu, E.Y.L., 'Dynamic systems analysis and control based on a configuration manifold model', *Nonlinear Dynamics* **19**, 2000, 113–134.

[23] Townley, S., 'Topological aspects of universal adaptive stabolization', *SIAM Journal of Control and Optimization* **34(3)**, 1996, 1044–1070.

[24] Ronki Lamooki, G. R., Townley, S., and Osinga, H. M., 'Normal forms, bifurcations and limit dynamics in adaptive control systems', *International Journal of Bifurcation and Chaos* **15(5)**, 2005, 1641–1664.

[25] Yang, L., *A modified model reference adaptive control algorithm to improve system robustness*, MSc Thesis, University of Bristol, 2004.

[26] Vinagre, B.M., Petrá, I., Podlubny, I., and Chen, Y.Q., 'Using fractional order adjustment rules and fractional order reference models in model-reference adaptive control', *Nonlinear Dynamics* **29**, 2002, 269–279.

[27] Rey, G. J., Johnson J, R., and Dasgupta, S., 'On tuning leakage for performance-robust adaptive-control', *IEEE Transactions on Automatic Control* **34(10)**, 1989, 1068–1071.

[28] Nascimento, V. H., and Sayed, A. H., 'Unbiased and stable leakage-based adaptive filters', *IEEE Transactions on Signal Processing* **47(12)**, 1999, 3261–3276.

[29] Carr, J., *Applications of centre manifold theory*, Springer-Verlag, 1981.